JOURNAL OF APPLIED PHYSICS **120**, 165305 (2016)

Factors influencing photoluminescence and photocarrier lifetime in CdSeTe/CdMgTe double heterostructures

C. H. Swartz,[1,a)] K. N. Zaunbrecher,[2] S. Sohal,[3] E. G. LeBlanc,[1] M. Edirisooriya,[1] O. S. Ogedengbe,[1] J. E. Petersen,[1] P. A. R. D. Jayathilaka,[1] T. H. Myers,[1] M. W. Holtz,[3] and T. M. Barnes[2]

[1]*Materials Science, Engineering, and Commercialization Program, Texas State University, 601 University Drive, San Marcos, Texas 78666, USA*
[2]*National Renewable Energy Laboratory, 15013 Denver West Parkway MS RSF200, Golden, Colorado 80401, USA*
[3]*Department of Physics, Texas State University, 601 University Drive, San Marcos, Texas 78666, USA*

(Received 11 August 2016; accepted 15 October 2016; published online 28 October 2016)

CdSeTe/CdMgTe double heterostructures were produced with both n-type and unintentionally doped absorber layers. Measurements of the dependence of photoluminescence intensity on excitation intensity were carried out, as well as measurements of time-resolved photoluminescence decay after an excitation pulse. It was found that decay times under very low photon injection conditions are dominated by a non-radiative Shockley-Read-Hall process described using a recombination center with an asymmetric capture cross section, where the cross section for holes is larger than that for electrons. As a result of the asymmetry, the center effectively extends photoluminescence decay by a hole trapping phenomenon. A reduction in electron capture cross section appeared at doping densities over 10^{16}cm^{-3}. An analysis of the excitation intensity dependence of room temperature photoluminescence revealed a strong relationship with doping concentration. This allows estimates of the carrier concentration to be made through a non-destructive optical method. Iodine was found to be an effective n-type dopant for CdTe, allowing controllable carrier concentrations without an increased rate of non-radiative recombination. *Published by AIP Publishing.*
[http://dx.doi.org/10.1063/1.4966574]

I. INTRODUCTION

CdTe solar cells continue to advance in both device performance and market share. Efficiency records for polycrystalline CdTe solar cells have recently exceeded 22% and continue to increase frequently.[1] This value remains well below the predicted Shockley–Queisser limit, suggesting that significant opportunities remain for improvement. Since the short-circuit current density is already near the theoretical limit, efforts are focusing on improving open-circuit voltage (V_{OC}) and fill factor, which are currently below 0.9 V and 80%, respectively, for most devices.[2] More effective doping is expected to increase the V_{OC}, and several recent efforts have demonstrated important improvements through longer carrier lifetime τ and low interface state density in single crystal CdTe.[3,4] These developments allow the electronic properties of CdTe to become comparable to those of GaAs, with the potential benefits of a slightly lower radiative recombination parameter and a higher tolerance to dislocations.

Efficient CdTe-based solar cells rely on the n-type layer to be much more heavily doped than the p-type absorber layer. Ideally, the p-side doping level should be several times larger than 10^{16} cm^{-3}, and the n-side should be well over an order of magnitude higher than this.[5] However, when using the industry's n-type dopants of choice, In and Cl, carrier lifetimes tend to degrade at these doping levels.[6,7] The photoluminescence (PL) for In-doped material is not dominated by an excitonic transition, suggesting that there are parasitic recombination pathways in CdTe:In.[8] However, Iodine doping was found to yield extremely bright excitonic photoluminescence (PL) at room temperature.[9] We therefore investigated iodine as an n-type dopant for CdTe layers.

Standard Hall effect measurements were used to measure the carrier concentration of doped samples grown on insulating substrates. This measurement, which is generally indispensable for doping studies, is necessarily destructive, and it is difficult to carry out on non-insulating substrates such as InSb. Making good Ohmic contacts to CdTe can itself be a non-trivial task.[10] Therefore, the dependence of photoluminescence intensity upon excitation intensity (PL-I), which has been used to monitor recombination-related energy levels and interface quality,[11] is proposed as a non-destructive means of estimating carrier concentration in samples with or without conducting substrates.

Throughout the doping range, a high minority carrier lifetime τ must be maintained.[12] The wider bandgap alloy $Cd_{1-x}Mg_xTe$ forms a type I heterojunction with CdTe, and it has the potential to serve as an electron-reflective buffer layer in CdTe-based solar cells.[13,14] Barriers made from this material have already proven highly effective at preventing the loss of photocarriers to the strong non-radiative recombination rates of bare CdTe surfaces.[15] Double Heterostructures (DHs), which enclose a CdTe film between two $Cd_{1-x}Mg_xTe$ barriers, can even serve as a model system for the study of the

[a)]Author to whom correspondence should be addressed. Electronic mail: craig.swartz@txstate.edu

optical properties of CdTe, in much the same fashion as GaAs/AlGaAs heterostructures.[16]

To quantify the lifetime, time-resolved photoluminescence (TRPL) measurements are typically employed. However, TRPL can sometimes be made ambiguous by multi-exponential traces.[17] These can be due to transport of photocarriers from their initial depth one absorption length from the top surface,[18] lateral transport from the laser excitation spot,[19] lateral transport into extended defects,[20] charge separation due to electric fields,[21] or a change in trap occupation with time.[22] By modeling both excitation-dependent and time-resolved PL, we find that the luminescence properties of the DHs studied are explicable in terms of a single non-radiative recombination center.

II. EXPERIMENT

For PL characterization, DHs were grown on (100) InSb substrates. InSb oxides were thermally desorbed under an antimony flux. A buffer layer of InSb was grown by molecular beam epitaxy (MBE) in a dedicated III-Sb chamber, which was followed by a buffer of $CdSe_yTe_{1-y}$. The weak selenium alloying of $y \sim 1\%$ is included to allow a full lattice match with the InSb. This approach is necessary to allow growth of samples greater than 2 μm on InSb substrates without misfit dislocations or any appreciable reduction in material quality.[23] The DH itself was then grown on this buffer, consisting of a 30 nm bottom barrier of CdMgTe, a 0.5–5 μm thick absorber layer of CdSeTe, and a top barrier of CdMgTe. A final 10 nm cap layer of CdTe was included to protect the Mg in the top barrier from oxidation in the ambient atmosphere.

In the double heterostructures, the bandgap (E_g) of the thin CdMgTe barriers was measured by variable angle spectroscopic ellipsometry (SE) in the range of 250–800 nm, at incident angles of 65°, 70°, and 75°. From E_g, the value of x could be found.[24] Samples were chosen with barrier Mg compositions of 33% and above. Low extended defect densities, of $10^5\,cm^{-2}$ or less, were verified by confocal PL microscopy. These measures helped to minimize the effect of the surface and dislocation density on the non-radiative recombination rate.

PL-I measurements used a 514 nm laser for excitation. A 6.5 × objective lens focused the laser light to a 120 μm FWHM Gaussian spot and collected the resulting PL, which was focused on a photomultiplier tube (PMT). The absolute excitation power could be varied with neutral density filters and measured with a calibrated power meter. TRPL was measured by time-correlated single photon detection using a 640 nm or 430 nm pulsed laser focused on a spot about 800 μm in diameter, yielding an injection level of 7×10^9 photons/cm^2 for a pulse. Note that this is a very low injection level, allowing observation of trap-related phenomena in TRPL. For electrical characterization, additional double heterostructures were grown on semi-insulating (211) or (100) CdTe substrates, without Se and beginning with a 200 nm CdTe buffer.[25] Simple 1–2 μm thick CdTe and $Cd_{1-x}Mg_xTe$ films were also grown on semi-insulating CdTe substrates. The Van der Pauw Hall effect technique was employed using soldered indium as a contact.

III. RESULTS

A. Analysis of TRPL lifetime

Figure 1 shows representative TRPL traces from DH samples with 640 nm excitation. Long TRPL decays are often observed at low excitation intensities, especially for undoped material. The extended signals are far above the background counts of the apparatus, and indeed two separate time-correlated TRPL setups at the National Renewable Energy Laboratory (NREL) and Texas State University (TSU) often yielded nearly identical extended traces using, respectively, 640 and 430 nm pulsed excitation.

Such long PL decays can occur when a center's minority carrier capture cross section is larger than its majority carrier capture cross section. In this case, the center becomes less effective as a Shockley-Read-Hall (SRH) recombination center and more effective as a carrier trap. After a photogeneration event, minority carriers rapidly fill the center. Since recombination by the capture of majority carriers is a

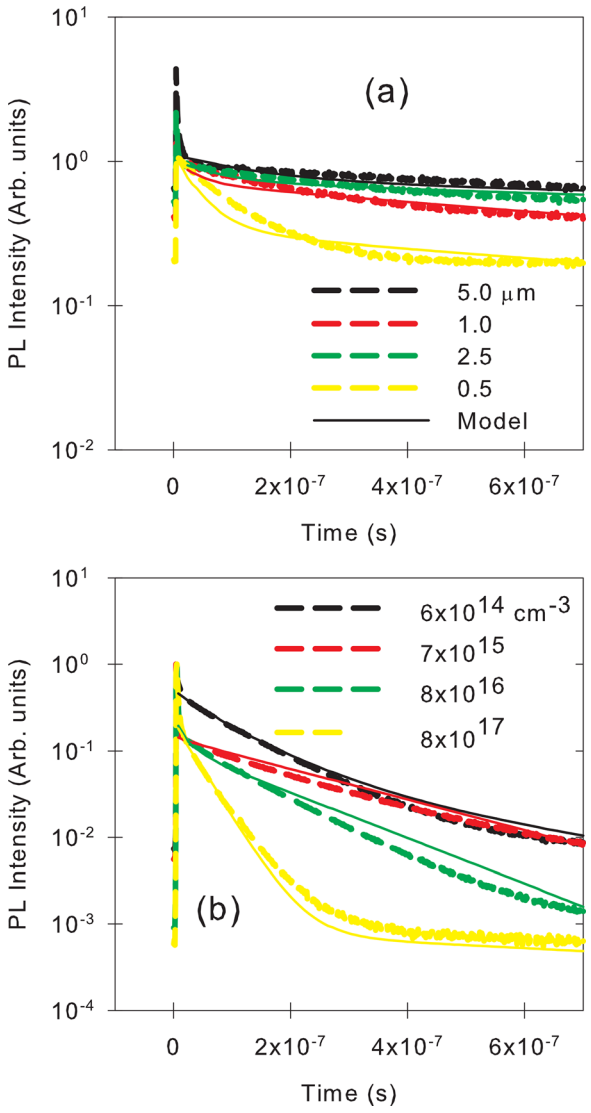

FIG. 1. TRPL traces shown for (a) undoped double heterostructures of several different thicknesses and (b) 1 μm thick samples of several different iodine doping concentrations. Each solid line represents a modeled time dependence.

slower process, the trapped carriers recombine at a relatively low rate, either by majority carrier capture or by first escaping through thermal emission. Those which escape thermally are able to recombine radiatively with majority carriers, producing the long PL signal.[22,26,27]

Given that the n-type materials in this study, shown in Fig. 1(b), can also sometimes exhibit a long PL decay within our measurement window, it is likely that there is a dominant trapping center with a higher hole capture cross section. Calculations undertaken by widely varied methods[28–30] have predicted that the Te_{Cd} antisite defect has a capture cross section for holes about an order of magnitude higher than that for electrons. Counterintuitively, the hole capture cross section remains higher even as coulomb forces attract electrons to the defect's positive charge state, while there is no corresponding negative charge state to attract holes.

We also note that in modeling layers with variable thickness, the photon recycling effect should be taken into account: photons released by radiative recombination are often reabsorbed within the film, re-forming the photocarrier pair.[31,32] The radiative recombination coefficient of CdTe material is $B^* = 1 \times 10^{-10}$ cm^3 s^{-1}. This can be found from the Van Roosbroeck-Shockley (VRS) relationship between absorption and recombination[33] by applying the absorption spectrum of CdTe.[34,35] While some experimental estimates of B^* have ranged an order of magnitude higher, recent studies analyzing PL-I coupled with TRPL on undoped DH strongly supported a lower value.[36] Recently, a study of phosphorus doping in bulk CdTe also strongly supported this value of B^*.[4]

Recycling further slows the net rate of radiative recombination with increasing thickness (d), leading to an effective radiative recombination coefficient of $B = (1-\gamma)B^*$. The thickness -dependent recycling factor γ was obtained by an optical modeling calculation which takes into account absorption and reflection.[37] The spectral dependence of radiated PL, indices of refraction, and absorption coefficients are included for CdTe.[38] Reflection from the InSb substrate can also be included, though its effect is negligible. As a result, an effective radiative recombination coefficient of about 25% of B^* should be used in a 1 μm thick CdTe heterostructure, as seen in Fig. 2. Note that only using the peak value of PL in a simplified calculation overestimates the recycling factor.

To model the effect of capture cross sections on TRPL, we begin by defining the maximum carrier rates of capture for holes in the case of entirely occupied traps, $1/\tau_p = \sigma_p v_{thp} N_t$, and for electrons in the case of entirely empty traps, $1/\tau_n = \sigma_n v_{thn} N_t$. For each carrier type, σ and v_{th} are the capture cross section and the thermal velocity. The TRPL trace may be viewed for simplicity as a three stage process: an initial very brief (<10 ns) drop in intensity is often observed which is related to the diffusion of the photocarriers from their initial location, one absorption length from the surface, to extend over the thickness of the heterostructure. In the second stage, the dominant cause of TRPL decay is the rapid capture of the photo-generated holes δp by traps, producing a decay rate of

$$\frac{1}{\tau_{2c}} = \frac{1}{\tau_p} F, \tag{1}$$

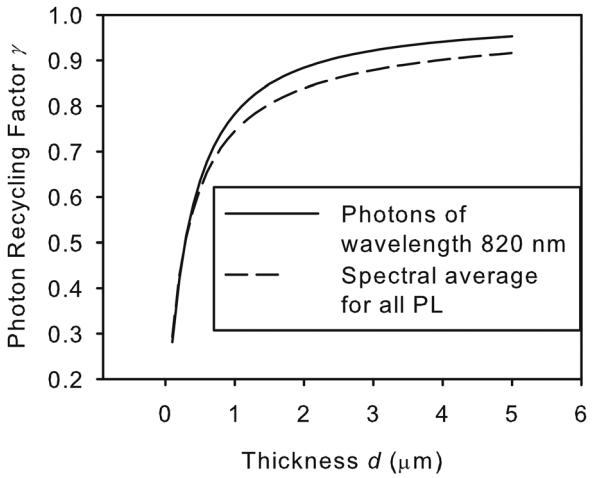

FIG. 2. The photon recycling factor for CdTe absorber layer as a function of thickness. The factor is also shown with the approximation of monochromatic PL emission at 820 nm.

where F is the fraction of traps occupied with electrons. For higher n-type doping, the radiative recombination rate $R_r = Bnp$ becomes more dominant in the second stage, where B is the effective radiative recombination coefficient, and the electron and hole concentrations are $n \cong N_D$ and p. In that case, the decay time would become

$$\frac{1}{\tau_{2r}} = Bn. \tag{2}$$

In the third stage, the PL signal is the result of holes escaping thermally from the trapping center and recombining directly with electrons. The decay rate is the result of a competition between the thermal emission of holes and non-radiative electron capture. The hole emission rate of an unoccupied trap is found from detailed balance considerations to be

$$\frac{1}{\tau_{3e}} = \frac{p_1}{\tau_p N_t}, \tag{3}$$

where the trap energy E_t, referenced to the valence band maximum, is included through the factor $p_1 = N_V \exp(-E_t/k_B T)$. Similarly, $n_1 = N_C \exp(-(E_g - E_t)/k_B T)$, where N_C and N_V are the conduction and valence band effective densities of states. Meanwhile, the electron capture rate of an unoccupied trap is

$$\frac{1}{\tau_{3c}} = \frac{1}{\tau_n}\frac{n}{N_t}. \tag{4}$$

Note that thermal emission is unlikely to create a detectable extended third PL stage unless the hole emission rate $1/\tau_{3e}$ is at least comparable to the non-radiative rate $1/\tau_{3c}$. Hence, a long secondary lifetime necessitates $1/\tau_{3e} \geq 1/\tau_{3c}$ or

$$\tau_n p_1 \geq \tau_p n, \tag{5}$$

which becomes a stringent requirement for more highly doped samples, where n approaches 10^{18} cm^{-3}. The most highly doped sample, shown in Fig. 1(b), does exhibit all three stages distinctly.

We carried out a numerical model for the TRPL and PL-I data in terms of trap parameters, as described in detail elsewhere.[16,36] Essentially, the equations relating the carrier concentrations, occupation probabilities, and capture rates are solved as a function of time after a pulsed excitation, or they are solved in steady state with a constant excitation. The solutions predict the dependence of radiative recombination $R_r = Bnp$ on excitation and time. The trap parameters N_t, E_t, σ_p, and σ_n are varied in a grid search method in order to reduce the error, or root mean square difference between the model and the data, for both TRPL and PL-I. For undoped material, changing a parameter by a factor of two typically results in the error increasing by more than a factor of three. For the two most heavily doped samples, the error was not as sensitive to the value of σ_n, which could be changed by an order of magnitude for a similar threefold increase in error.

The modeling of the TRPL indicates that results from the full range of doping and thickness can be explained by a dominant trap with an energy of $E_t = 0.3\,\text{eV}$ above the valence band and a hole capture cross section of $\sigma_p = 4 \times 10^{-15}$ cm^2. The remaining parameters are summarized in Table I, while the model results are compared with the TRPL data in Fig. 1 and the PL-I data in Fig. 3. The trap density is expressed as sheet density $N_{ts} = d\,N_t$. The observation that N_{ts} remains constant over a wide range of thicknesses indicates the trapping is occurring at an interface rather than representing bulk recombination/trapping sites. The drop in σ_n at higher doping densities is a consequence of screening that we will discuss in Sec. III-B.

We can also use these trap parameters to roughly estimate the TRPL results without numerical modeling. The trace is approximated as a series of discrete stages occurring in a homogeneous sample with both excitation and trap density uniformly distributed. The traps are situated lower in the bandgap, and so we assume they begin as mostly occupied so that $F \sim 1$. Such a multi-stage estimate ignores several other effects which can only be included by numerical computation, such as the rate of holes which are repeatedly emitted and then recaptured by traps in the third stage, with the capture rate given in Equation (1), and the fact that F is continually varying with time.

From Equation (1), we see that the undoped traces in Fig. 1(a) would have a second stage decay rate of $1/\tau_{2c} = 1/\tau_p$. Using Table I, the thinnest undoped sample has a rate of $1/\tau_p = N_t \sigma_p v_{thp} = (2 \times 10^{14}\text{cm}^{-3})\ (4 \times 10^{-15}\ \text{cm}^2)\ (10^7\text{cm/s}) \sim 8 \times 10^6\text{s}^{-1}$, which is about the same as the slope in the first 200 ns of TRPL data. In a similar way, the second stage lifetimes seen on the TRPL traces in Fig. 1(a) can be estimated by varying N_t. In the third stage, electron capture is negligible, resulting in the greatly decreased emission-based decay rate of Equation (3).

For the doped samples, the second stage decay rate gains the addition of BN_D from Equation (2), in agreement with the increased second stage slope for the highest doped sample in Figure 1(b). The final decay rate gains the addition of the electron capture rate of $N_D \sigma_n v_{thn}$ from Equation (4), which is most significant for the samples doped at 7×10^{15}

TABLE I. Parameters for the model results in Figs. 1 and 3. In all cases, the trap energy is $E_t = 0.3\,\text{eV}$ above the valence band maximum, and the hole capture cross section is $\sigma_p = 4 \times 10^{-15}$ cm^2. The absorber thickness is given by d.

N_D (cm^{-3})	d (μm)	N_{ts} (cm^{-2})	σ_n (cm^2)
0	5	2×10^{10}	3×10^{-16}
0	2.5	1×10^{10}	3×10^{-16}
0	1	1×10^{10}	3×10^{-16}
0	0.5	1×10^{10}	3×10^{-16}
6×10^{14}	1	1×10^{10}	3×10^{-16}
7×10^{15}	1	1×10^{10}	4×10^{-16}
8×10^{16}	1	3×10^{10}	6×10^{-18}
8×10^{17}	1	2×10^{10}	1×10^{-19}

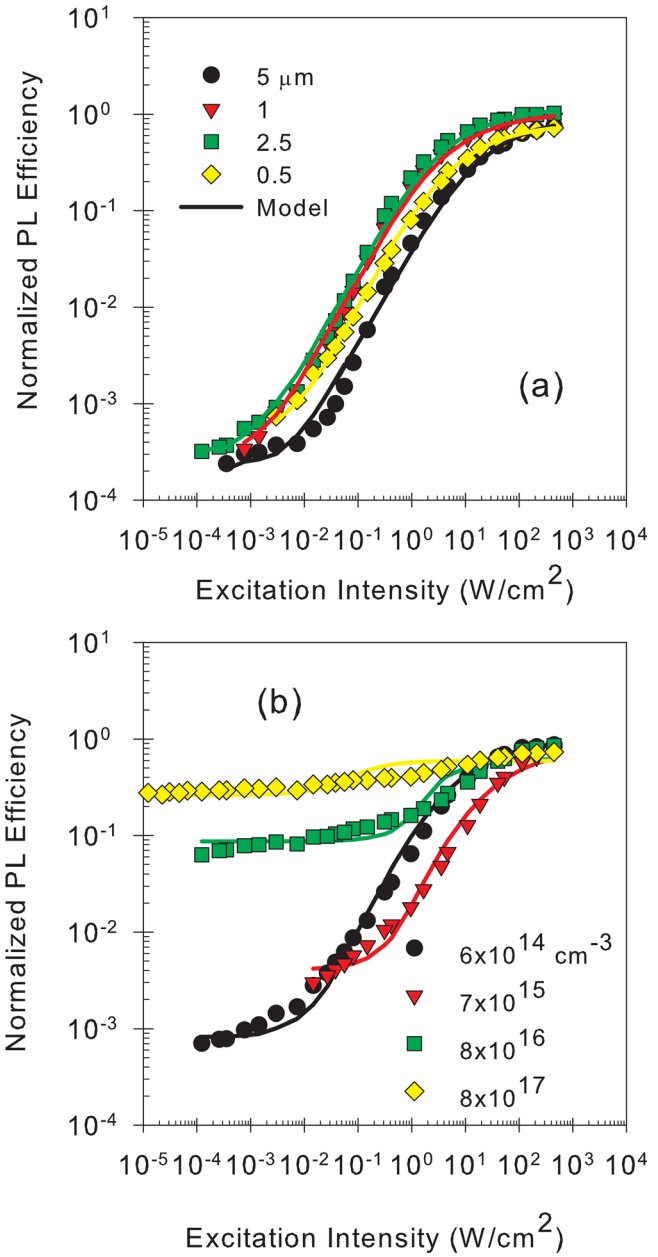

FIG. 3. Ratio of PL intensity to laser excitation incident at the sample surface (I), plotted as a function of the excitation, for (a) undoped double heterostructures of several different thicknesses and (b) 1 μm thick samples of several different iodine doping concentrations. Each solid line represents a modeled intensity dependence.

and $8 \times 10^{16}\,\mathrm{cm}^{-3}$, in agreement with the more rapid final decay in those two samples. The electron capture rate is on the order of $10^{7}\,\mathrm{s}^{-1}$ for these two samples while the measured final decay is somewhat slower, suggesting that the numerical solution is needed for a more quantitative agreement. The final decay rate for the most heavily doped sample, at $8 \times 10^{17}\,\mathrm{cm}^{-3}$, is markedly slowed by the screening-related reduction in σ_n.

Finally, excitation pulses that are strong enough for the number of photocarriers to exceed the number of traps ($\delta p \gg FN_t$) will leave enough holes in the valence band to render thermal trap escape an insignificant source of PL signal. This accounts for an observed quenching of the extended decay within our measurement time window when the excitation power was increased to 1×10^{11} photons/cm^2 per pulse. Thus in order to probe the minority carrier lifetime, rather than the trapping phenomenon here, one must investigate an injection regime high enough to quench the interface traps and yet within the low injection range where the minority carrier lifetime retains its meaning.

B. Analysis of PL intensity

The PL intensity was also examined in steady state. In Fig. 3, typical PL-I results show the normalized efficiency, or the emission intensity divided by excitation intensity (I), as a function of I. Higher doping concentration leads to generally higher luminescence efficiency at lower excitation, as would be expected from the dependence of the radiative recombination rate R_r on carrier concentration. The rate scales with electron and hole concentration as $R_r = Bnp$. The fact that PL intensity does not degrade at the $10^{18}\,\mathrm{cm}^{-3}$ iodine doping level compares favorably with equivalent indium doping levels.[7]

With higher I, the contribution of radiative recombination increases and the radiative efficiency ultimately approaches 100%. Note that the step-like relationship between efficiency and I decreases in magnitude with increased doping. This relationship can provide information on trap characteristics and even doping level. As mentioned previously, the PL-I measurements can be explained using the parameters found in Table I. Again, a single trap adequately explains the observed behavior, as indicated by the lines in Fig. 3.

We can quantify the magnitude of the step by finding the maximum slope of the PL-I relationship, S_{max}. As we will show, this gives an alternate, non-destructive technique for estimating doping level. In doped material, we first note that the radiative recombination rate is

$$R_r = Bnp \cong BN_D p. \tag{6}$$

In steady state, the excitation rate is equal to the total recombination rate, including the trap-related SRH contribution,[39]

$$I = R_{tot} = R_r + \frac{np}{\tau_p(n+n_1) + \tau_n(p+p_1)} \cong BN_D p + \frac{N_D p}{\tau_p(N_D+n_1) + \tau_n(p+p_1)}. \tag{7}$$

The slope on a log scale is therefore

$$S(p) = \frac{d\,\log(R_r/I)}{d\,\log(I)} = \frac{R_{tot}}{R_r}\frac{dR_r/dp}{dI/dp} - 1. \tag{8}$$

The maximum slope is found by solving

$$\frac{dS(p)}{dp} = 0, \tag{9}$$

for p to obtain

$$p_{max} = \frac{\sqrt{B_{nt}(B_{nt}+1)}}{B(\tau_n+\tau_p)}, \tag{10}$$

where the dimensionless quantity

$$B_{nt} \equiv B\tau_p(N_D+n_1) + B\tau_n(p_1), \tag{11}$$

is defined. Finally, solving $S(p_{max}) = S_{max}$ for B_{nt}, we have

$$B_{nt} = \frac{1}{4S_{max}(1+S_{max})}. \tag{12}$$

Taking the maximum PL-I slope (S_{max}) from each sample's experimental data, B_{nt} can be calculated. To derive S_{max} in a robust way, the data may be put through a least squares fit to an empirical sigmoidal function $f(I) = f_0 + a/[1+\exp((I_0-I)/b)]$ with the free parameters f_0, I_0, a, and b. After this, the maximum slope is easily obtained as $a/(4b)$. By estimating the carrier concentration n from Hall effect measurements on identically doped samples grown on CdTe (100) substrates, calculated values of B_{nt} are found to depend on n as shown in Fig. 4.

Fitting the data in Fig. 4 on a linear scale results in a slope of 4×10^{-18} cm^3. Based on the definition in Equation (11), this slope is equal to $B\tau_p$, suggesting a value of 160 ns for τ_p. While there can be little doubt that the density of unintentional defects N_t, and hence τ_p, will vary somewhat from growth to growth, the TRPL results suggested a value within a factor of two, or $\tau_p = 250$ ns, for 1 μm thick undoped layers.

The lifetime τ_p is sufficiently constant that B_{nt} varies approximately linearly with N_D, even as low as $N_D = 10^{16}\,\mathrm{cm}^{-3}$, where Ohmic contact formation is very difficult. Therefore, if a PL signal is strong enough that it is practical to find the maximum slope in its excitation dependence (S_{max}), then the value of n may be found provided that the $B_{nt}(n)$ relationship is known, either by calibrating the relationship through Hall effect measurements on several samples or by knowledge of the dominant trap's parameters obtained from some other source, such as TRPL.

The linear scale offset of B_{nt} is 0.1–0.2 in the limit of $N_D = 0$. The same value of B_{nt} appears in samples that are unintentionally doped. From Equation (11), we see that $B\tau_n p_1 = 0.1$–0.2, since n_1 is negligible for trap energies near the valence band. The product $\tau_n p_1$ must therefore be less than 5×10^{9} s cm^{-3} for low doped samples. However, extended PL decay with a doping density of $8 \times 10^{17}\,\mathrm{cm}^{-3}$ requires from Equation (5) that the product $\tau_n p_1$ is greater than 2×10^{11} s cm^{-3}, at least for more heavily doped samples.

This factor of 40 discrepancy between the values of $\tau_n p_1$ at heavy and light doping might at first suggest that a new set

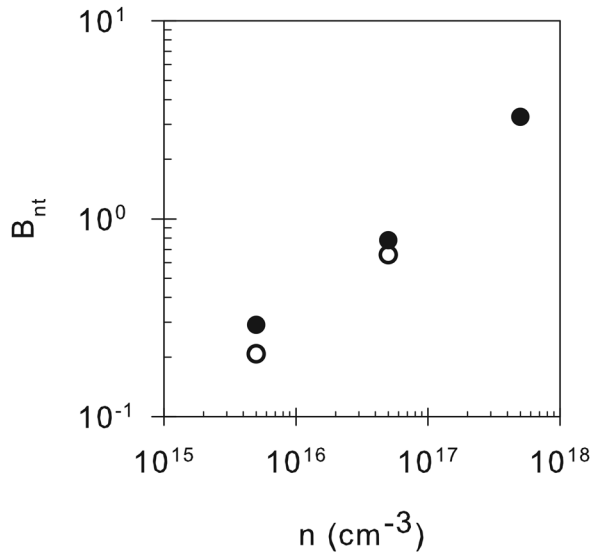

FIG. 4. The quantities B_{nt}, calculated from the maximum slopes in Fig. 3, are plotted vs. carrier concentration in DHs with 1 μm (filled) and 2 μm (empty) CdTeSe absorber layers.

of SRH centers, with different energies, cross sections, and concentrations, is potentially being induced by iodine doping. However, the results throughout the range of doping concentrations can be explained by a single center with a variation in electron capture cross section with doping density. The capture cross section of an attractively charged trap is expected to fall rapidly with carrier concentration as the screening length drops under five times the effective Bohr radius of a charged center.[40] Given the electron effective mass and dielectric constant in CdTe,[41] the screening length in nm is $\lambda = 3.9 \times 10^9/n^{1/2}$, with n expressed in units of cm^{-3}, while the effective Bohr radius is $a_0^* = 5.9$ nm. This implies a rapid reduction in electron capture cross section for $N_D > 10^{16}\,cm^{-3}$, which is consistent with the σ_n required to fit the doped TRPL and PL-I data, as seen in Table I.

The energy and hole capture cross section values are comparable to the values of $E_t = 0.34$ eV and $\sigma_p = 8$–10×10^{-15} cm^2 which are often reported for hole traps in CdTe and CdTeSe using current transient spectroscopy (CTS) techniques.[42,43] Some example theoretical predictions for the Te_{Cd} defect were of $E_t = 0.4$ eV, with $\sigma_p = 7 \times 10^{-14}$ cm^2 for $Te_{Cd}{}^+$, and $\sigma_n = 8 \times 10^{-15}$ cm^2 for $Te_{Cd}{}^{+2}$.[29] The theoretically predicted asymmetry in cross sections is seen in this study, although the cross section values are smaller than the predicted values. The latter may be due in part to the coulomb repulsion of the positive charge state, which was not considered for the hole capture mechanism. In theoretical calculations, screening would not cause much of a reduction in hole capture, since the effective Bohr radius for holes is one order of magnitude smaller, meaning that N_D must be two orders of magnitude greater for the screening to be as effective.

It remains uncertain if the trap seen in this study is indeed the native defect Te_{Cd} or if other interfacial states are responsible, there remains a long-standing tendency for non-radiative recombination to be reduced in thicker heterostructures.[32] The observation that the trap concentration is relatively insensitive to thickness, when expressed as a sheet density as given in Table I, supports an interface-related trap. It is also possible that native defects such as Te_{Cd} form more often near interfaces.

IV. CONCLUSIONS

For well-passivated heterostructures, the carrier concentration of a given film can be estimated in a non-destructive way over a very wide range from an analysis of the dependence of PL intensity upon excitation intensity, resulting in a non-destructive and contactless method for determining carrier concentration.

Measured TRPL lifetimes, even during the rapid early decay stages, often surpass the theoretical limit $\tau_{rad} = 1/(BN_D)$ for radiative recombination in material with a given doping level, even with the more recent lower value of radiative coefficient B accounted for. This is consistent with the photon recycling effect, similar to what is observed for doped GaAs/AlGaAs DHs, underscoring that once surface recombination is controlled, the optoelectronic properties of CdTe are comparable to those of GaAs. An accurate knowledge of the photon recycling factor is also a requirement for analyzing PL measurements.

Measured TRPL lifetimes do not always easily yield the minority carrier lifetime. The measured lifetimes in single crystal material may be extended by a hole trap level with an asymmetric capture cross section. Prior modeling calculations[16] were based upon the industry standard assumption that the capture cross sections are 10^{-15} cm^2 for holes and 10^{-12} cm^2 for electrons.[44] However, the PL characteristics appear to require a much smaller cross section for electrons, and the further reduction of the cross section by screening effects at higher doping levels. Both steady-state and transient PL measurements can be adequately explained by a single SRH center with an asymmetric capture cross section consistent with that predicted for the native defect Te_{Cd}.

ACKNOWLEDGMENTS

Funding from the Alliance for Sustainable Energy, LLC, the manager and operator of the National Renewable Energy Laboratory for the U.S. Department of Energy. Contract No. DEAC36-08GO28308 FPACE II: Approaching the S-Q Limit with Epitaxial CdTe, Subcontract No. ZEJ-4-42007-0.

[1]M. A. Green, K. Emery, Y. Hishikawa, W. Warta, and E. D. Dunlop, Prog. Photovoltaics **22**, 701 (2014).
[2]T. A. Gessert, S. H. Wei, J. Ma, D. S. Albin, R. G. Dhere, J. N. Duenow, D. Kuciauskas, A. Kanevce, T. M. Barnes, J. M. Burst, W. L. Rance, M. O. Reese, and H. R. Moutinho, Sol. Energy Mater. Sol. Cells **119**, 149 (2013).
[3]J. N. Duenow, J. M. Burst, D. S. Albin, D. Kuciauskas, S. W. Johnston, R. C. Reedy, and W. K. Metzger, Appl. Phys. Lett. **105**, 053903 (2014).
[4]J. M. Burst, J. N. Duenow, D. S. Albin, E. Colegrove, M. O. Reese, J. A. Aguiar, C. S. Jiang, M. K. Patel, M. M. Al-Jassim, D. Kuciauskas, S. Swain, T. Ablekim, K. G. Lynn, and W. K. Metzger, Nat. Energy **1**, 16015 (2016).
[5]R. Scheer and H. W. Schock, *Chalcogenide Photovoltaics: Physics, Technologies, and Thin Film Devices* (Wiley-VCH, Weinheim, Germany, 2011), pp. 137–145.
[6]M. Turker, J. Kronenberg, M. Deicher, H. Wolf, and T. Wichert, Hyperfine Interact. **177**, 103 (2007).

[7]X. H. Zhao, S. Liu, Y. Zhao, C. M. Campbell, M. B. Lassise, Y. S. Kuo, and Y. H. Zhang, in *IEEE 42nd Photovoltaic Specialist Conference*, New Orleans, LA, 14–19 June 2015 (IEEE, Danvers, MA, 2015), p. 768.
[8]W. Palosz, K. Grasza, P. R. Boyd, Y. Cui, G. Wright, U. N. Roy, and A. Burger, J. Electron. Mater. **32**, 747 (2003).
[9]N. C. Giles, J. Lee, T. H. Myers, Z. H. Yu, B. K. Wagner, R. G. Benz, and C. J. Summers, J. Electron. Mater. **24**, 691 (1995).
[10]B. Ghosh, Microelectron. Eng. **86**, 2187 (2009).
[11]M. Passlack, R. N. Legge, D. Convey, Z. Y. Yu, and J. K. Abrokwah, IEEE Trans. Instrum. Meas. **47**, 1362 (1998).
[12]M. Gloeckler and J. R. Sites, Thin Solid Films **480**, 241 (2005).
[13]Y. S. Kuo, J. Becker, S. Liu, Y. Zhao, X. H. Zhao, P. Y. Su, I. Bhat, and Y. H. Zhang, in *IEEE 42nd Photovoltaic Specialist Conference*, New Orleans, LA, 14–19 June 2015 (IEEE, Danvers, MA, 2015), p. 62.
[14]T. Song, A. Kanevce, and J. R. Sites, IEEE J. Photovoltaics **5**, 1762 (2015).
[15]M. J. DiNezza, X. H. Zhao, S. Liu, A. P. Kirk, and Y. H. Zhang, Appl. Phys. Lett. **103**, 193901 (2013).
[16]C. H. Swartz, M. Edirisooriya, E. G. LeBlanc, O. C. Noriega, P. A. R. D. Jayathilaka, O. S. Ogedengbe, B. L. Hancock, M. Holtz, T. H. Myers, and K. N. Zaunbrecher, Appl. Phys. Lett. **105**, 222107 (2014).
[17]R. K. Ahrenkiel, B. M. Keyes, D. L. Levi, K. Emery, T. L. Chu, and S. S. Chu, Appl. Phys. Lett. **64**, 2879 (1994).
[18]W. K. Metzger, R. K. Ahrenkiel, J. Dashdorj, and D. J. Friedman, Phys. Rev. B **71**, 035301 (2005).
[19]A. Kanevce, D. Kuciauskas, D. H. Levi, A. M. Allende Motz, and S. W. Johnston, J. Appl. Phys. **118**, 045709 (2015).
[20]B. Fluegel, K. Alberi, M. J. DiNezza, S. Liu, Y. H. Zhang, and A. Mascarenhas, Phys. Rev. Appl. **2**, 034010 (2014).
[21]W. K. Metzger, D. Albin, D. Levi, P. Sheldon, X. Li, B. M. Keyes, and R. K. Ahrenkiel, J. Appl. Phys. **94**, 3549 (2003).
[22]J. S. Blakemore, *Semiconductor Statistics* (Dover, New York, 1987), pp. 274–277.
[23]C. H. Swartz, M. Edirisooriya, O. S. Ogedengbe, B. L. Hancock, S. Sohal, E. G. LeBlanc, P. Jayathilaka, O. C. Noriega, M. Holtz, T. H. Myers, and K. N. Zaunbrecher, in *IEEE 42nd Photovoltaic Specialist Conference*, New Orleans, LA, 14–19 June 2015 (IEEE, Danvers, MA, 2015), p. 532.
[24]S. G. Choi, Y. D. Kim, S. D. Yoo, D. E. Aspnes, I. Miotkowski, and A. K. Ramdas, Appl. Phys. Lett. **71**, 249 (1997).
[25]K.-K. Lee and T. H. Myers, J. Vac. Sci. Technol., A **33**, 031602 (2015).
[26]R. K. Ahrenkiel, B. M. Keyes, and D. J. Dunlavy, J. Appl. Phys. **70**, 225 (1991).
[27]M. Maiberg, T. Hoelscher, S. Zahedi-Azad, and R. Scheer, J. Appl. Phys. **118**, 105701 (2015).
[28]C. Buurma, S. Krishnamurthy, and S. Sivananthan, J. Appl. Phys. **116**, 013102 (2014).
[29]D. N. Krasikov, A. V. Scherbinin, A. A. Knizhnik, A. N. Vasiliev, B. V. Potapkin, and T. J. Sommerer, J. Appl. Phys. **119**, 085706 (2016).
[30]J.-H. Yang, L. Shi, L.-W. Wang, and S.-H. Wei, Sci. Rep. **6**, 21712 (2016).
[31]S. M. Durbin, J. L. Gray, R. K. Ahrenkiel, and D. H. Levi, in *IEEE 23rd IEEE Photovoltaic Specialists Conference*, Louisville, KY, 10–14 May 1993 (IEEE, Danvers, MA, 1993), p. 628.
[32]X. H. Zhao, M. J. DiNezza, S. Liu, C. M. Campbell, Y. Zhao, and Y. H. Zhang, Appl. Phys. Lett. **105**, 252101 (2014).
[33]W. Vanroosbroeck and W. Shockley, Phys. Rev. **94**, 1558 (1954).
[34]A. P. Kirk, M. J. DiNezza, S. Liu, X. H. Zhao, and Y. H. Zhang, in *IEEE 39th Photovoltaic Specialists Conference*, Tampa, FL, 16–21 June 2013 (Danvers, MA, 2013), p. 2515.
[35]A. E. Rakhshani, J. Appl. Phys. **81**, 7988 (1997).
[36]C. H. Swartz, O. C. Noriega, P. A. R. D. Jayathilaka, M. Edirisooriya, X. H. Zhao, M. J. DiNezza, S. Liu, Y. H. Zhang, and T. H. Myers, in *IEEE 40th Photovoltaic Specialist Conference*, June 8–13 2014 (IEEE, Daners, MA, 2014), p. 2419.
[37]M. A. Steiner, J. F. Geisz, I. García, D. J. Friedman, A. Duda, and S. R. Kurtz, J. Appl. Phys. **113**, 123109 (2013).
[38]S. Adachi, T. Kimura, and N. Suzuki, J. Appl. Phys. **74**, 3435 (1993).
[39]S. M. Sze and K. K. Ng, *Physics of Semiconductor Devices*, 3rd ed. (Wiley-Interscience, Hoboken, USA, 2006), pp. 42–45.
[40]O. Z. Alekperov, J. Phys.: Condens. Matter **10**, 8517 (1998).
[41]O. Madelung, *Semiconductors: Data Handbook*, 3rd ed. (Springer-Verlag, Heidelburg, Germany, 2004), pp. 232–234.
[42]H. Elhadidy, J. Franc, P. Moravec, P. Hoeschl, and M. Fiederle, Semicond. Sci. Technol. **22**, 537 (2007).
[43]R. Gul, U. N. Roy, S. U. Egarievwe, A. E. Bolotnikov, G. S. Camarda, Y. Cui, A. Hossain, G. Yang, and R. B. James, J. Appl. Phys. **119**, 025702 (2016).
[44]M. Gloeckler, A. L. Fahrenbruch, and J. R. Sites, in *Proceedings of 3rd World Conference on Photovoltaic Energy Conversion*, Osaka, Japan, 11–18 May 2003 (IEEE, Danvers, MA, 2003), p. 491.